



Artificial neural network model for the flow regime recognition in the drying of guava pieces in the spouted bed

Yago Matheus da Silva Veloso, Marcello Maia de Almeida, Odelsia Leonor Sanchez de Alsina & Manuela Souza Leite

To cite this article: Yago Matheus da Silva Veloso, Marcello Maia de Almeida, Odelsia Leonor Sanchez de Alsina & Manuela Souza Leite (2019): Artificial neural network model for the flow regime recognition in the drying of guava pieces in the spouted bed, Chemical Engineering Communications, DOI: [10.1080/00986445.2019.1608192](https://doi.org/10.1080/00986445.2019.1608192)

To link to this article: <https://doi.org/10.1080/00986445.2019.1608192>



Published online: 29 Apr 2019.



Submit your article to this journal [↗](#)



View Crossmark data [↗](#)



Artificial neural network model for the flow regime recognition in the drying of guava pieces in the spouted bed

Yago Matheus da Silva Veloso^a, Marcello Maia de Almeida^b, Odelsia Leonor Sanchez de Alsina^a, and Manuela Souza Leite^a

^aInstitute of Technology and Research, Tiradentes University (UNIT), Aracaju, Sergipe, Brazil; ^bDepartment of Environmental and Sanitary Engineering, State University of Paraiba, Campina Grande, Paraíba, Brazil

ABSTRACT

In this article, an artificial neural network model (ANN) was developed for the flow regime recognition in the spouted bed dryer. Instabilities and changes were observed in the hydrodynamics of the bed during the drying of guava pieces with deformability and variation in physical properties. Changes in the Archimedes number and Littman parameter directly affected the hydrodynamics of the bed. Experimental data on the variation of the properties of the dried guava pieces were used to obtain the fluid dynamics parameters this was also used as an input data in the ANN model whereas the operating regime of the spouted bed dryer, fixed-, fluidized-, spouted-, and slugging beds were the output model variables. The architecture of the neural network model was selected using the particle swarm optimization algorithm (PSO). The optimized neural model achieved a recognition accuracy of 86% for the fixed and fluidized beds and 99% for the spouted and slugging beds.

KEYWORDS

ANN; Deformable particles; Drying process; Mathematical modeling; Nonlinear process; Particle swarm optimization; Spouted bed

Introduction

Drying is one of the most important and oldest methods to maintain the quality of food stuffs. Drying process consists of the removal of water from the solid material to an acceptable lower moisture content by simultaneous transfer of heat and mass in the solid and gas phases. The stability of the regime can be analyzed through the Archimedes number and Littman parameter, fluid dynamics parameters that depend on the particles, and the fluid properties, which directly affect the behavior of the bed (Mathur and Epstein, 1974).

During the drying of deformable solid particles in the spouted bed dryer, it was observed that the material shrinks and their physical properties vary, in turn causing bed instabilities and changes in the flow regimes (Hatamipour and Mowla, 2002).

One strategy to avoid such changes in the hydrodynamics of the bed would be a control system application of operational variables of the

dryer. For the development of this system, it is necessary to have a prior knowledge about the variation of the flow regimes during drying so that the actuators of the control system can make anticipated decisions and avoid instabilities and flow regime changes in the bed (Almeida et al., 2006).

In a composite system of solids and gases, the regime observation depends on the characteristics of the bed particles, the geometry of the spouted bed dryer, and the operating conditions. The spouting occurs in a certain air velocity range. With an increase in the air velocity, many flow regimes can be observed in the bed system, such as fixed bed, fluidization, incipient spouting, pulsating spouting, and spouted and slugging bed. Du et al. (2015) detected four flow regimes, including fixed-, spouted-, bubbling-, and slug-ging-bed, in a cylindrical spouted bed. Xu et al. (2014) identified five flow regimes, namely fixed bed, spouting, spouting with slugging, bubbling, and agitated bed, in a semi-cylindrical spouted bed with a conical base, whereas Wang et al.

(2011b) observed four flow regimes, namely fixed bed, stable spouting, bubbling, and slugging.

The conventional method for recognizing the flow regime in a spouted bed dryer is visual observation, as noted in the papers of Dogan et al. (2004) and Freitas et al. (2000). Some papers in the literature cite the study conducted on the fluidization of deformable solid particles, such as pieces of potato, green beans, and peas (Senadeera et al., 2000; 2003; Palzer et al., 2012). However, visual observation is not possible on an industrial scale equipment (Wang et al., 2011a). Due to this problem, different authors developed different techniques to recognize these regimes in the spouted bed dryer (Xie et al., 2004; Wang et al., 2012).

The artificial neural network (ANN) is a heuristic soft computing method widely used for modeling the nonlinear and complex systems seen in various branches of science (Leite et al., 2011; Santos et al., 2012; Oliveira et al., 2015). The ANN model was used to predict the variation in the physical properties of various types of materials while drying (Kerdpi boon et al., 2006; Mihajlovic et al., 2011; Aghbashlo et al., 2015; Silva et al., 2015) and for recognizing the flow regimes used as input data pressure fluctuation signals in the bed during drying (Mi et al., 2001; Xie et al., 2004). This recognition method can be used not only in gas-solid systems but also in gas-liquid systems or even multiphase systems (gas-solid-liquid; Xie et al., 2004; Wang et al., 2011a). However, no study applying the ANN in the recognition of flow regimes during the drying of deformable solid particles could be found in the literature.

In this article, experimental data of the drying of pieces of guava in a spouted bed were used (Almeida et al., 2006), including the data of the variations of physical properties during the drying. These data were used as input variables in the ANN model development in order to predict the flow regimes during the drying process.

Experimental system

The spouted bed dryer system consists of a plexi-glass conical cylindrical column and the dryer wall allows visual observation of the changes that

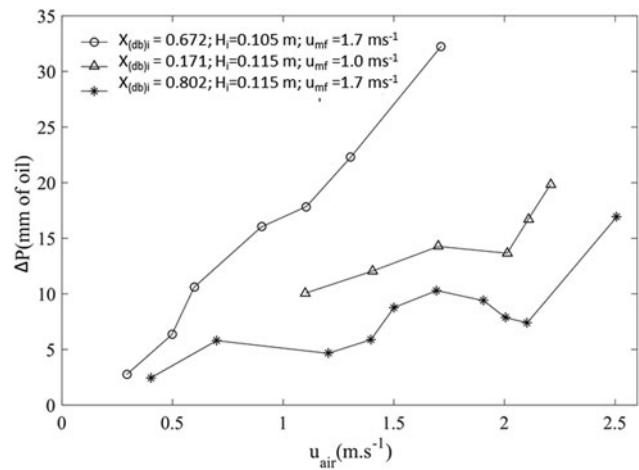


Figure 1. Characteristic curve for the bed cubic pieces of guava in the spouted bed dryer at different levels of moisture content and bed height.

take place in the flow regimes during drying. The column has 1 m height, 10.8 cm internal diameter, and 4.6 mm thickness; the conical base was 9 cm tall and had an internal angle of 60°; and the diameter of spout nozzle was 2.8 cm. The experimental apparatus was completed with an air supply system, that included a blower (model S100L2, 4 hp, 2920 rpm, Eberle), a rotameter (model R.2.V.C, capacity of 400 m³ h⁻¹, Omel), and a flow control valve (globe valve, Emerson). The pressure drops (Δp) in the bed was measured by a “U” type manometer, filled with oil (density 0.86 g cm⁻³). Later, this variable was expressed as mm of oil in Figure 1.

The particles used for drying in the spouted bed were cubic pieces of guava, which shows important variation of their physical properties during drying. The fact that pieces of guava lose moisture and suffer shrinkage and rounding by attrition during drying directly influences the behavior of the physical properties, which in turn affects the hydrodynamics of the bed. The particle bed, constituted by the pieces of guava, was classified as group C according to Geldart (1973). Thus, these particles are presented as spoutable but with an unstable behavior, in most cases.

The cubic pieces of the guava were obtained using the mesocarp of the fruit after being cleaned, peeled, and withdrawn to its seeds. Then, particles with a thickness between 0.2 and 1.5 cm were obtained using a stainless-steel cutter. The initial moisture content of the pieces of

guava were about 4.75 kg of water/kg of dry solid (dry base); it was necessary to pre-dry it in a fixed bed in order to adjust the moisture content levels of these particles to levels that allowed their processing in the spouted bed (between 0.6 and 1.5 kg of water/kg of dry solid). The shapes of the particles were initially approximately cubic with rounded vertices, which modified during drying to become almost spherical. This resultant geometric form was assumed for modeling purpose.

The operational conditions that were tested were initial bed height (H_i) of 0.09 to 0.12 m, air drying velocity (u_{air}) of 2.8 to 3.5 m.s⁻¹, and initial moisture content (dry base) of 0.6 to 1.5 for the guava pieces ($X_{(\text{db})i}$), while the air drying temperature in the spouted bed was set at 60 °C.

Samples of the bed particles (about 2 g) were collected in order to characterize the particles, at fixed time intervals. The moisture of the pieces of guava was determined by gravimetric method using the oven Marconi Model MA035/2 with air circulation at 70 °C for 24 h. The density was determined by the liquid pycnometer method using absolute ethyl alcohol PA Vetec and the mean particle diameter was determined using displaced liquid volume by a known number of particles for sphere equivalent volume. Details about experimental apparatus and procedure could be found elsewhere (Almeida et al., 2006).

The Archimedes number (Ar) and the Littman parameter (A) were determined due to the loss of moisture content of the pieces of guava and the consequent variation in the particle diameter (d_p) and particle density (ρ_p) according to Equations (1) and (2), respectively. The changes in the physical properties of the pieces of guava directly affected these dimensionless numbers and, consequently, the stability of the dryer flow regime.

$$Ar = d_p^3 g \rho_{\text{air}} (\rho_p - \rho_{\text{air}}) / \mu^2 \quad (1)$$

$$A = \rho_{\text{air}} u_{\text{mf}} u_t / (\rho_p - \rho_{\text{air}}) g d_o \quad (2)$$

whereas d_o is the diameter of the fluid inlet nozzle, g is the gravity acceleration, u_{mf} is the superficial velocity at minimum fluidization, u_t is the terminal velocity of the particle, ρ_{air} is the air-drying density, and μ is the air drying viscosity.

Visual observations of the drying of the pieces of guava in the spouted bed dryer were made to analyze the characteristics of the particle

circulation within the bed and to classify the regimes as fixed bed, fluidization, spouted bed, and slugging. These observations were made as a function of the drying time and the bed flow regime maps were obtained using the different experimental conditions that were tested (Almeida et al., 2006).

Development of neural model for recognition of flow regimes

A database containing 180 samples were made with the aim of guaranteeing comprehensiveness about the problem (Ameer et al., 2017) and improving the prediction capacity of the model. Data were randomly separated into subsets—70% for training, 15% for validation, and 15% for network model tests. This separation of data was defined as it was reported in the literature. The training data set was prepared from minimum and maximum values of the variables. The early stopping (based on cross-validation method) was used to detect when overfitting starts during supervised training of a neural network; training is then stopped before convergence to avoid the overfitting, which is the loss of generalization capacity of the neural model. The input data were normalized to values of -1 and $+1$ using Equation (3). The output data were coded by means of dummies because this data followed the qualitative data type while the original variables were transformed into artificial ones to be used in the estimation of models that indicate the absence or presence of attributes. The MATLAB neural network toolbox was used for the development of the predictive model. The Softmax function was used in the neural network because it was classificatory and represented the probability of the data being one of the defined classes. The backpropagation Levenberg–Marquardt was defined as a training algorithm. For training, validation, and testing of the network, the mean squared error (MSE) and root mean squared error (RMSE) were used as indicators of performance of the model, according to Equations (4) and (5).

$$Y = (y_{\text{max}} - y_{\text{min}}) (x - x_{\text{min}}) / (x_{\text{max}} - x_{\text{min}}) + y_{\text{min}} \quad (3)$$

$$\text{MSE} = \sum (y_{\text{calc}} - y_{\text{exp}})^2 / n \quad (4)$$

$$\text{RMSE} = \sqrt{\sum (y_{\text{icalc}} - y_{\text{iexp}})^2 / n} \quad (5)$$

According to Equations (3)–(5): y_{max} is equal to 1, y_{min} is equal to -1 , x_{max} is the maximum value that the variable can assume, x_{min} is the minimum value that the variable to be normalized can assume, x is the value of the variable that is intended to be normalized, y_{iexp} is the real value obtained experimentally, y_{icalc} is the value obtained using the neural model, and n is the number of samples.

The particle swarm optimization (PSO) algorithm was used to select the number of neurons in the intermediate layer and to transfer the function between the input and intermediate layer, and the ideal learning rate. This search algorithm aims to find the best solution within the universe of possible solutions and is based on the individual and collective behavior of the flocks of birds in search of food. The position and velocity of the particles are updated at each iteration until the entire cluster converges to obtain the best result (Alam et al., 2014; Das et al., 2014; Kalani et al., 2017; Viana et al., 2018). Equations (6) and (7) were used to determine the velocity and position of each particle in the swarm at each iteration.

$$v_{i(t+1)} = w \cdot v_{i(t)} + c_1 r_1 (y_i(t) - x_i(t)) + c_2 r_2 (y_i(t) - x_i(t)) \quad (6)$$

$$x_i(t+1) = x_i(t) + v_i(t+1) \quad (7)$$

In Equations (6) and (7), $v_i(t)$ is the particle velocity in the iteration t , $x_i(t)$ is the position of the particle in the iteration t , w is the inertial weight, and c_1 and c_2 are the personal and global coefficient of the acceleration, respectively. The terms r_1 and r_2 are variables that assume aleatory values at each iteration and, thus, have the function of making the influence of the individual and global terms in the speed equation random. $y_i(t)$ refers to the best overall position within the particle swarm and also represents the best position of particle i .

The transfer functions tested during the training phase between the input layer and the intermediate layer of the ANN architecture were linear, hyperbolic tangent, and sigmoid logarithm functions, as given in Equations (8)–(10), where n is the numbers of input, a is the sigmoid function slope parameter,

Table 1. Input and output variables of the neural model for flow regime recognition.

Variables	Ranges
<i>Input</i>	
Ar	$6.2 \times 10^6 - 1.83 \times 10^7$
A	0.096–0.132
u_{air} (m.s ⁻¹)	2.8–3.5
<i>Output</i>	
Flow regime	Fixed bed-Slugging

and y is the output value of the function.

$$y(n) = n \quad (8)$$

$$y(n) = (2/(1 + \exp^{-2n})) - 1 \quad (9)$$

$$y(n) = 1/(1 + \exp^{-an}) \quad (10)$$

Results

Characteristic curve and spout stability

Diced pieces of guava at different levels of moisture content in dry bases ($X_{d,b}$: 17.1, 67.2, and 80.2%, respectively) and bed height (H_i : 0.105 and 0.115 m) were used to evaluate the hydrodynamics of the spouted bed dryer.

It was observed that as the airdrying velocity increases, the bed with pieces of guava rises as a whole without an expansion and the bottom of the bed was fluidized in diluted form while the bed surface was fluidized homogeneously. For higher airdrying velocity, the bed was fluidized in a stationary manner, which is characteristic of systems consisting of large particles.

Figure 1 shows the characteristic curve of the pieces of guava in the spouted bed dryer. It was noticed that the characteristic curves do not present the usual trend found in conventional spouted beds. This could be attributed to the changes in the particle properties during the data acquisition due to the deformable nature of the material. It was verified that the behavior of the curve in the region of minimum fluidization was complex by rapidly passing the bed to another flow regime. In high velocity, the bed presented slugging as expected for the coarse particles bed.

PSO-ANN modeling

The developed neural model had the Littman parameter (A), Archimedes number (Ar), and the airdrying velocity (u_{air}) as input variables and the flow regime as an output variable. The ranges of

the variables used as input and output of the neural model in the flow regime recognition are described in Table 1.

The PSO parameter algorithm (c_1 , c_2 , and number of particle) was selected to analyze the MSE, which was chosen as the objective function. The personal and global coefficient of the acceleration (c_1 and c_2) corresponded to the acceleration that helped each particle in the swarm to search for personal and global best positions. The number of particles in the swarm determined the size of the space covered by the problem (Zendehboudi et al., 2012). The initial and final value of the evaluated c_1 and c_2 were 1.4 to 2.6 and the numbers of particles were 15 to 25. The goal of the PSO algorithm was to minimize the MSE.

The results of the PSO-ANN training that uses different values of c_1 and c_2 and different numbers of particles in the swarm is shown in Figure 2. It was noted that the best configuration of the PSO were obtained for the $c_1 = 2.2$ and $c_2 = 25$ particles in the swarm. The best configuration of the PSO allowed the obtainment of MSE and RMSE values of 0.0128 and 0.113.

The ideal architecture configuration of the neural network was determined using the PSO optimization algorithm with the accuracy value of the flow regime recognition obtained after each training process. Table 2 shows the variations of the parameter of the neural model optimized using the PSO algorithm.

Figure 3 illustrates the network architecture of the final model for the recognition of bed flow regimes during the drying of the guava pieces. Figure 4 shows the evaluation of the MSE performance index as a function of the number of iterations in the neural model. It was noticed that with each iteration of the developed model, the value of MSE decreased and that after 17 iterations, there was a decrease in the training error while the validation error increased, which signifies overtraining in the later epochs (Kumar et al., 2008). The optimized neural model obtained the MSE value and RMSE values equal to 0.0297 and 0.172, respectively.

The recognition accuracy of the four flow regimes observed in the spouted bed by the ANN model for

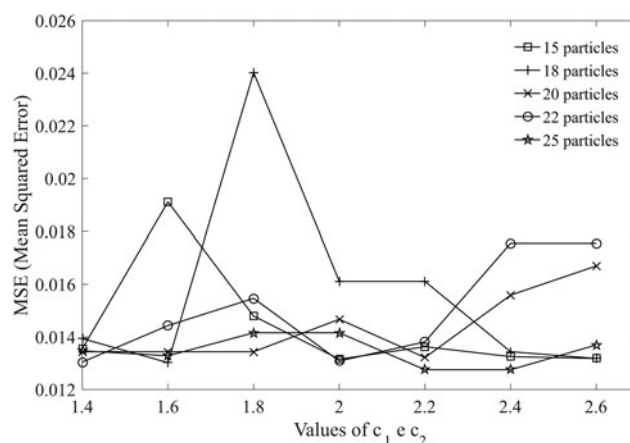


Figure 2. Effects of the c_1 and c_2 values and the numbers of particles in PSO-ANN model performance (MSE).

the databases used in the different stages of development of the model are shown in Figure 5.

In Figure 5, the main diagonal of each matrix represents the number of right recognitions made for each flow regimes (1- fixed bed, 2- fluidization, 3- spouted bed, and 4- slugging). The sum of all the percentages of right recognition for the four regimes are presented in the last line of the last column of the matrix; in this square, the right percentage is given above, while the number written below denotes the wrong or forgotten recognition percentage. The squares above and below the main diagonal of the matrix shows the numbers of classifications made incorrectly. It was noticed that in the databases of training, validation, testing, and all data, the neural model obtained recognition efficiency for the four flow regimes equal to 96.8, 96.3, 81.5, and 94.4%, respectively.

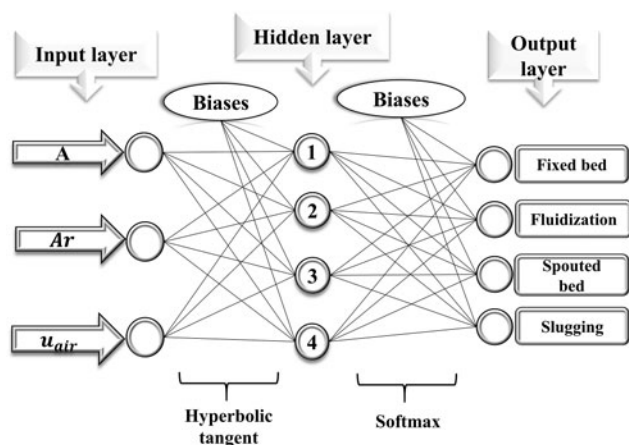
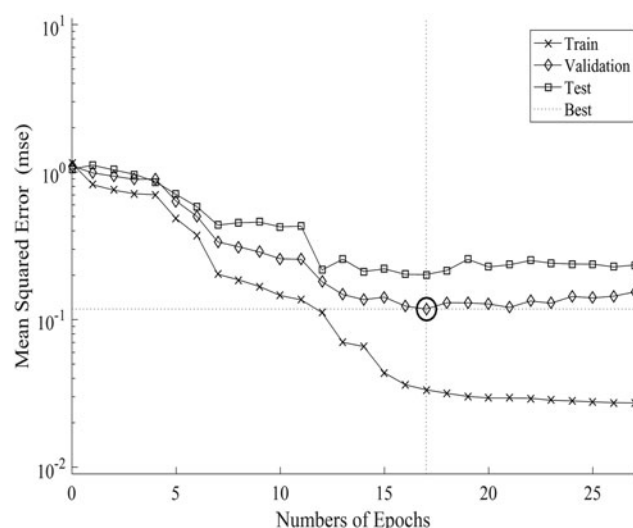
Table 3 presents the weight and biases of the neural model developed, where W_i and B_1 refers to the weights and biases of the input layer and the intermediate layer neurons and W_o and B_2 refers to the weights and biases of the intermediate layer and output layer neurons.

Using the developed ANN model, tests were carried out using the model to verify the efficiency of the flow regime recognition in the spouted bed in different operational conditions of the drying.

Figures 6(a-c) illustrates the comparisons made between the experimentally observed flow regimes (Almeida et al., 2006) and those predicted by the neural model for different experimental conditions over the drying time. In these

Table 2. Neural model parameters optimized using PSO algorithm.

Parameters	Variation	Optimized parameter
Numbers of neurons	1–7	4
Transfer function in the intermediate layer	Linear, hyperbolic tangent, and logarithmic sigmoid	Hyperbolic tangent
Learning rate	0–1	0.24

**Figure 3.** Optimized architecture of the neural model for the flow regime recognition in the spouted bed dryer.**Figure 4.** Performance of the MSE value obtained by the neural model as a function of the numbers of epochs using training, validation, and testing.

charts, the experimental visualization transitions are represented by the dashed vertical lines whereas the predicted regimes by the ANN model are represented by the chart markers.

It can be seen in Figures 6(a–c) that the classification of the flow regimes using the neural model was successful. The predictions made by the model for each of the regimes were, almost on every occasion, within the range established for each regime, according to experimental determination.

Table 4 presents the accuracy of the neural model for the recognition of the four (4) flow regimes observed in the drying of diced guava pieces in the spouted bed dryer. Note that the regimes that showed the highest classification errors were fixed bed and fluidization. What may better explain the misclassification in these regimes is the fact that these regimes are in close proximity to the transition flow regime. The same behavior was reported in studies found in the literature, where the authors reported that there were greater errors in the recognition of flow regimes in the plug flow regime and a strong agitation, considered by the authors as transition flow regimes (Xie et al., 2003).

The results presented in Table 4 shows the efficient accuracy of the neural model in the recognition of flow regimes. In studies in literature, where models were based on recurrent neural networks and support vector machines and pressure fluctuation signals in the spouted bed were used as input data of the model, it was reported that accuracies obtained were between 80 and 90% (Wang et al., 2011; 2012). Thus, the model developed in this work presented greater efficiency in the recognition of flow regimes than the models developed in previous studies. It is also worth noting that the model was efficient in predicting the regimes even when tested under different operational conditions.

Thus, it was proved that the models based on artificial neural networks constitute an efficient method of recognition of flow regimes in spouted bed dryers using operating parameters of the bed as the drying air velocity (u_{air}) and fluid dynamic parameters (A , Ar) as input variables, which vary according to the physical properties of the particles, that can be applied in the equipment of industrial scale.

The application of these models to industrial spouted bed dryers can increase the efficiency of the drying process by taking into account several events, such as the dead zones formation in the bed or sudden changes in the fluid dynamics behavior, such as elevation of the height of the

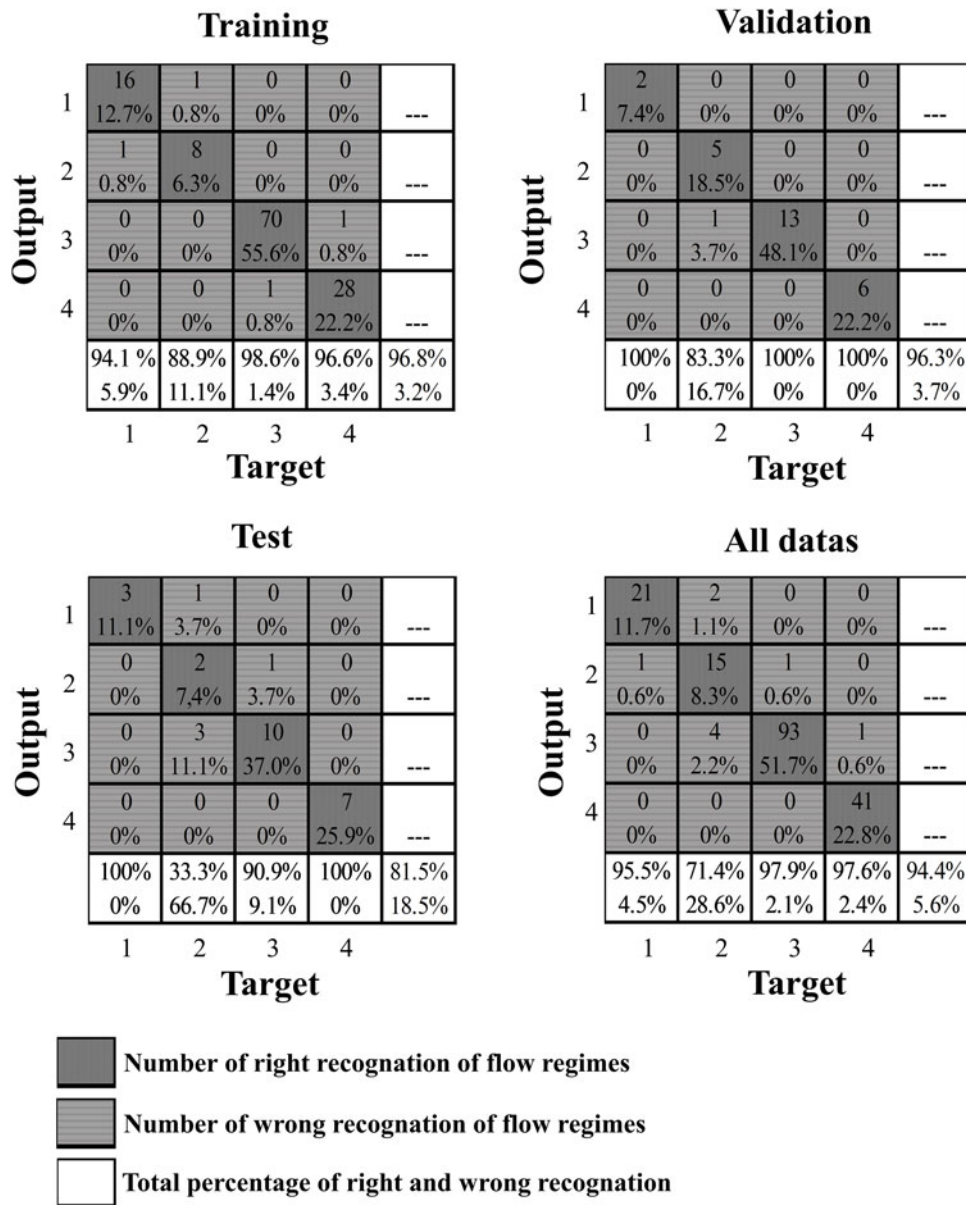


Figure 5. The recognition accuracy of the four flow regimes (1- fixed bed, 2- fluidization, 3- spouted bed, and 4- slugging) for the training, validation, test, and all databases.

Table 3. Weight and biases matrix for the developed model.

Neurons	W_i				W_o				
	Input variables			Biases (B_1)	Output variables				Biases (B_2)
	A	Ar	u_{air}		Fixed bed	Fluidization	Spouted bed	Slugging	
1	-0.49	-5.71	-0.17	0.70	-4.10	4.03	0.60	-0.29	1.07
2	-5.54	-3.75	4.78	3.16	-3.35	-2.07	3.57	1.36	0.87
3	-11.45	-3.87	-1.78	-12.5	-3.24	-5.78	-5.55	16.55	-3.27
4	4.32	5.92	2.94	-1.51	1.20	3.57	-3.79	-1.37	0.47

fountain accompanied by sudden changes in pressure, or until the spout collapses. These oscillations in the regimes and changes in the stability during the drying process cause a decrease in the efficiency of the process.

Conclusion

An ANN model was developed for the recognition of the flow regimes in the drying of guava pieces in the spouted bed. Such material has the characteristic of deformability during drying and

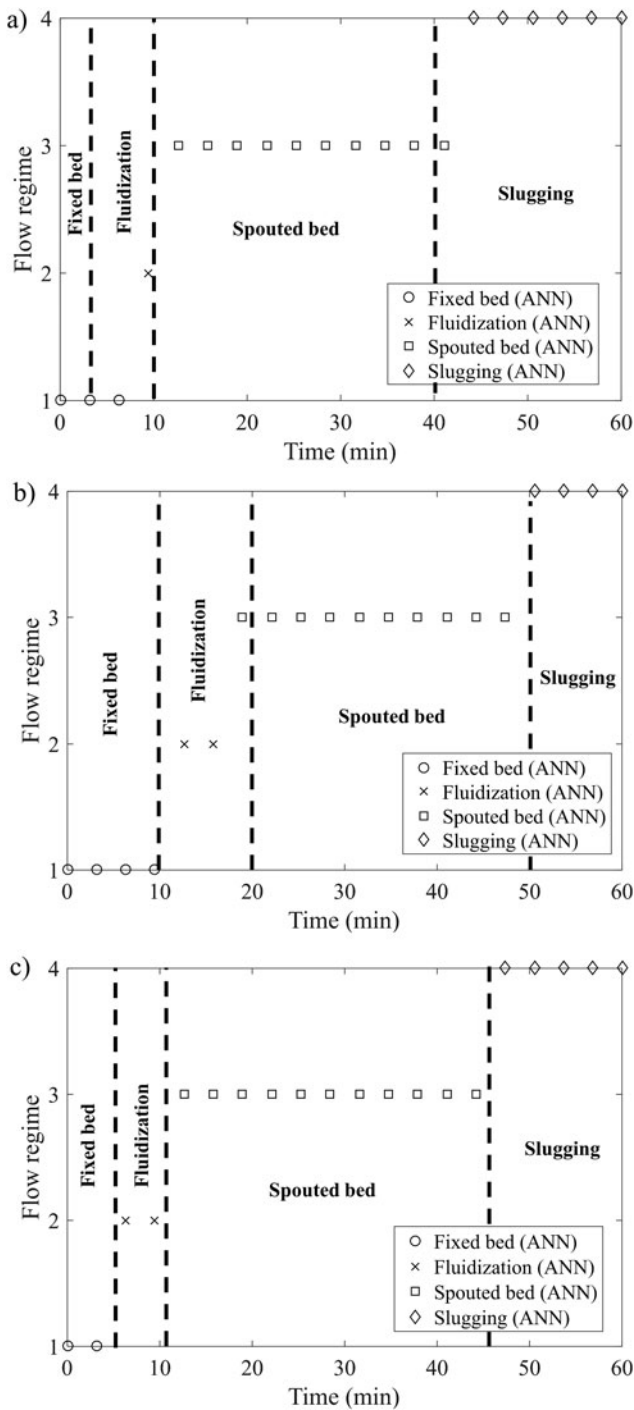


Figure 6. Recognition of the flow regime visually and predicted by the ANN model: (a) $H_i = 0.09$ m, $X_{(db)i} = 1.5$ and $u_{air} = 3.5$ m.s⁻¹; (b) $H_i = 0.12$ m, $X_{(db)i} = 1.5$, and $u_{air} = 3.5$ m.s⁻¹; and (c) $H_i = 0.105$ m, $X_{(db)i} = 1.05$, and $u_{air} = 3.2$ m.s⁻¹.

directly influences the stability and changes in flow regimes. The developed neural model was able to identify the changes in the flow regimes, using operational parameters of the dryer, such as drying air velocity, and fluid dynamics

Table 4. Accuracy of recognition of the different flow regimes observed during the drying of pieces of guava in the spouted bed dryer.

Flow regime	Accuracy of recognition (%)
Fixed bed	86.0
Fluidization	86.0
Spouted bed	99.0
Slugging	99.9

parameters (A , Ar), as input data. The developed neural network was optimized using the PSO, in which the best configuration of the neural network architecture was selected using a hidden layer containing four neurons, hyperbolic tangent, Softmax transfer functions, and a learning rate equal to 0.24 (MSE = 0.0128 and RMSE = 0.113). The neural model achieved a recognition accuracy of 86% in fixed bed and fluidization regimes, 99% in spouted bed, and 99.9% in slugging regimes. The satisfactory performance of the neural network model demonstrates that this flow rate recognition technique is promising and can be used in industrial dryers in order to avoid the loss of process efficiency due to instability and changes in flow regimes.

Acknowledgement

The authors acknowledge the support of CAPES and FAPITEC/SE.

Nomenclature

μ	air drying viscosity (kg.m ⁻¹ .s ⁻¹)
A	Littman parameter (–)
Ar	Archimedes number (–)
c_1	personal acceleration coefficient
c_2	global acceleration coefficient
d_o	fluid inlet nozzle diameter (m)
d_p	particles diameter (m)
g	gravity acceleration (m.s ⁻²)
H_i	initial bed height (m)
r_1	acceleration coefficient (variable that assume random values in the range (0–1))
r_2	acceleration coefficient (variable that assume random values in the range (0–1))
u_{air}	air drying velocity (m.s ⁻¹)
u_{mf}	superficial velocity at minimum fluidization (m.s ⁻¹)
u_t	terminal velocity of the particle (m.s ⁻¹)
v_i	particle velocity;
w	inertial weight;
X_{db}	moisture content (dry base)
x_i	position of the particle;

y_i	best position of the particle;
ρ_{air}	air drying density (kg.m^{-3})
ρ_p	particle density (kg.m^{-3})

References

- Aghbashlo, M., Hosseinpour, S., and Mujumdar, A. S. (2015). Application of artificial neural networks (ANNs) in drying technology: A comprehensive review, *Dry. Technol.*, **33**, 1397–1462.
- Alam, S., Dobbie, G., Koh, Y. S., Riddle, P., and Ur Rehman, S. (2014). Research on particle swarm optimization based clustering: A systematic review of literature and techniques, *Swarm. Evol. Comput.*, **17**, 1–13.
- Almeida, M. M., Silva, O. S., and Alsina, O. L. S. (2006). Fluid-dynamic study of deformable materials in spouted-bed dryer, *Dry. Technol.* **24**, 499–508.
- Ameer, K., Bae, S. W., Jo, Y., Lee, H. G., Ameer, A., and Kwon, J. H. (2017). Optimization of microwave-assisted extraction of total extract, stevioside and rebaudioside-A from *Stevia rebaudiana* (bertoni) leaves, using response surface methodology (RSM) and artificial neural network (ANN) modelling, *Food Chem.*, **229**, 198–207.
- Das, G., Pattnaik, P. K., and Padhy, S. K. (2014). Artificial neural network trained by particle swarm optimization for non-linear channel equalization, *Expert Syst. Appl.*, **41**, 3491–3496.
- Dogan, Ö. M., Uysal, B. Z., and Grace, J. R. (2004). Hydrodynamic studies in a half slot-rectangular spouted bed column, *Chem. Eng. Commun.*, **191**, 566–579.
- Du, W., Zhang, L., Zhang, B., Bao, S., Xu, J., Wei, W., and Bao, X. (2015). Flow regime transition and hydrodynamics of spouted beds with binary mixtures, *Powder Technol.*, **281**, 138–150.
- Freitas, L. A. P., Dogan, O. M., Lim, C. J., Grace, J. R., and Luo, B. (2000). Hydrodynamics and stability of slot-rectangular spouted beds part II: Increasing bed thickness, *Chem. Eng. Commun.*, **181**, 243–258.
- Geldart, D. (1973). Types of gas fluidization, *Powder Technol.*, **7**, 285–292.
- Hatamipour, M. S., and Mowla, D. (2002). Shrinkage of carrots during drying in an inert medium fluidized bed, *J. Food. Eng.*, **55**, 247–252.
- Kalani, H., Sardarabadi, M., and Passandideh-Fard, M. (2017). Using artificial neural network models and particle swarm optimization for manner prediction of a photovoltaic thermal nanofluid based collector, *Appl. Therm. Eng.*, **113**, 1170–1177.
- Kerdpiroon, S., Kerr, W. L., and Devahastin, S. (2006). Neural network prediction of physical property changes of dried carrot as a function of fractal dimension and moisture content, *Food Res. Int.*, **39**, 1110–1118.
- Kumar, K. V., Porkodi, K., Rondon, R. L. A., and Rocha, F. (2008). Neural network modeling and simulation of the solid/liquid activated carbon adsorption process, *Ind. Eng. Chem. Res.*, **47**, 486–490.
- Leite, M. S., Santos, B. F., Lona, L. M. F., Silva, F. V., and Fileti, A. M. F. (2011). Application of artificial intelligence techniques for temperature prediction in a polymerization process, *Chem. Eng. Trans.*, **24**, 385–390.
- Mathur, K. B., and Epstein, N. (1974). *Spouted Beds*, Academic Press, New York, 1955.
- Mi, Y., Ishii, M., and Tsoukalas, L. H. (2001). Flow regime identification methodology with neural networks and two-phase flow models, *Nucl. Eng. Des.*, **204**, 87–100.
- Mihajlovic, T., Ibric, S., and Mladenovic, A. (2011). Application of design of experiments and multilayer perceptron neural network in optimization of the Spray-Drying process, *Dry. Technol.*, **29**, 1638–1647.
- Oliveira, G. R., Santos, A. V., Lima, A. S., Soares, C. M. F., and Leite, M. S. (2015). Neural modeling in adsorption column of cholesterol-removal efficiency from milk, *LWT - Food Sci. Technol.*, **64**, 632–638.
- Palzer, S., Dubois, C., and Gianfrancesco, A. (2012). Generation of product structures during drying of food products, *Dry. Technol.*, **30**, 97–105.
- Santos, B., Leite, M., Silva, F., and Fileti, A. (2012). Neural network model predictive control of a styrene polymerization plant: Online testing using an electronic worksheet, *Chem. Pap.*, **66**, 654–663.
- Senadeera, W., Bhandari, B. R., Young, G., and Wijesinghe, B. (2003). Influence of shapes of selected vegetable materials on drying kinetics during fluidized bed drying, *J. Food Eng.*, **58**, 277–283.
- Senadeera, W., Bhandari, B., Young, G., and Wijesinghe, B. (2000). Physical properties and fluidization behaviour of fresh green bean particulates during fluidized bed drying, *Food Bioprod. Process*, **78**, 43–47.
- Silva, B. G., Fileti, A. M. F., and Taranto, O. P. (2015). Drying of Brazilian pepper-tree fruits (*Schinus terebinthifolius* Raddi): Development of classical models and artificial neural network approach, *Chem. Eng. Commun.*, **202**, 1089–1097.
- Viana, D. F., Salazar-Banda, G. R., and Leite, M. S. (2018). Electrochemical degradation of reactive black 5 with surface response and artificial neural networks optimization models, *Sep. Sci. Technol.*, **53**, 2647–2661.
- Wang, C., Zhong, Z., and Jiaqiang, E. (2012). Flow regime recognition in spouted bed based on recurrence plot method, *Powder Technol.*, **219**, 20–28.
- Wang, C., Zhong, Z., and Li, R. (2011a). Flow regime recognition in the spouted bed based on Hilbert-Huang transformation, *Korean J. Chem. Eng.*, **28**, 308–313.
- Wang, C., Zhong, Z., Li, R., and Jia-Qiang, E. (2011b). Recognition of the flow regimes in the spouted bed based on fuzzy c -means clustering, *Powder Technol.*, **205**, 201–207.
- Xie, T., Ghiaasiaan, S. M., and Karrila, S. (2003). Flow regime identification in gas/liquid/pulp fiber slurry flows based on pressure fluctuations using artificial neural networks, *Ind. Eng. Chem. Res.*, **42**, 7017–7024.
- Xie, T., Ghiaasiaan, S. M., and Karrila, S. (2004). Artificial neural network approach for flow regime classification in

- gas-liquid-fiber flows based on frequency domain analysis of pressure signals, *Chem. Eng. Sci.*, **59**, 2241–2251.
- Xu, H., Zhong, W., Jin, B., and Wang, J. (2014). Flow pattern and transition in gas-liquid-solid three phase spouted bed, *Powder Technol.*, **267**, 18–25.
- Zendehboudi, S., Ahmadi, M. A., James, L., and Chatzis, I. (2012). Prediction of condensate-to-Gas ratio for retrograde gas condensate reservoirs using artificial neural network with particle swarm optimization, *Energy Fuels*, **26**, 3432–3447.